APPLICATION OF FILAMENT WINDING TECHNOLOGY FOR CS22 CATEGORY WING CONSTRUCTION

Jakub Cejpek **Michal Mališ** **Tomáš Urík**

Brno University of Technology, Institue of aerospace engineering

Technicka 2896/2, 616 69 Brno, Czech republic

y100957@stud.fme.vutbr.cz malis@fme.vutbr.cz urik@fme.vutbr.cz

Abstract. The classical conception of a wing inner construction for CS-22 category is the spar construction. Spar is loaded by normal force and the bending moment, whereas the skin is loaded by the torque. On the opposite side, the shell wing construction is distributing the entire load through the skin.

For many years the technology of filament winding has been used to create high quality shell constructions such as fuselage segments or rocket combustion chambers. This technology achieves favourable strength/weight and stiffness/weight ratios as well as manufacturing reproduction.

The CompoTech Plus, s.r.o. company owns the know-how in the area of tubes filament winding (cylinders for hydraulic and pneumatic systems, beams of an agricultural sprayer machines or mobile radio towers).

In cooperation with the HpH, s.r.o. sailplane manufacturer started a project, which aims to investigate the possibility of appalling the filament winding technology in wing production. The first stage of the project is to suggest a wing construction and evaluate the stress in each part of the suggested construction. Based on this analysis a real test wing segment would be manufactured and tested.

The design and testing would take place at the Institute of aerospace engineering, Brno University of technology.

Keywords. Filament winding, wing, shell construction, spar, beam, carbon fiber.

1 Introduction

The precise fibre placement is used by large manufacturers like Boeing for winding fuselage segments for some time. This article investigates the possibilities of using this kind of technology for manufacturing small airplane structures, in this case CS22 category wing.

GS304 is a sailplane manufactured by HpH company. Several wing segments were tested under static and dynamic loading in the test room at Institute of Aerospace Engineering, Brno University of Technology. These test serve as reference data during parametric design of the wound wing segment.

The objective of this study is to suggest, analyze, produce and test wound wing segment. There are technologies available nowadays that allow to accomplish this task relatively cheaply and in a short period of time. The technologies available will affect the materials and design approaches used.

For winding is used large automated machine at Compotech company. HpH company owns CNC milling machine that is suitable and affordable for complete milling of the foam core.

The authors expect that this study will contribute to the development of the low-cost CS22 category airplane manufacturing. It is hoped that manufacturing that uses precise placement technology will make the manufacturing faster, more precise, more effective. The automated fibre placement will diminish the human-error and increase the mechanical properties of the final product.

1.1 Expectations and known issues

The filament placement is almost fully machine-operated process, thus reducing human errors in layup quality. The repeatability and productivity is ensured by computer program of the winding process. The exact layup promises possible gain in mechanical strength.
While creating the first variant of the wound segment, the technology could create only one kind of layup (constant thickness) along the wing span. This problem however has been eliminated later (after first segment was already manufactured).

1.2 Segment geometry

The original inner structure (Fig. 1 and 2), designed by HpH, is classical spar and rib construction. The main spar ends with cantilever (connects right and left wing, Fig. 2, position 3&4). The fuselage is connected through the root rib, which includes two pins (Fig. 2, positions 1&2).

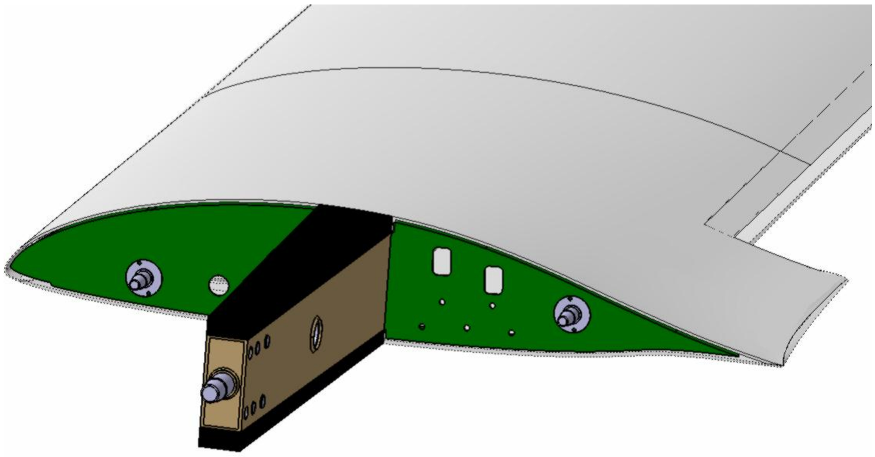

Figure 1: HpH wing structure.

The wing segment is 3800mm long, excluding the cantilever (600mm). The root chord is 855mm and chord at the tip is 600mm long.

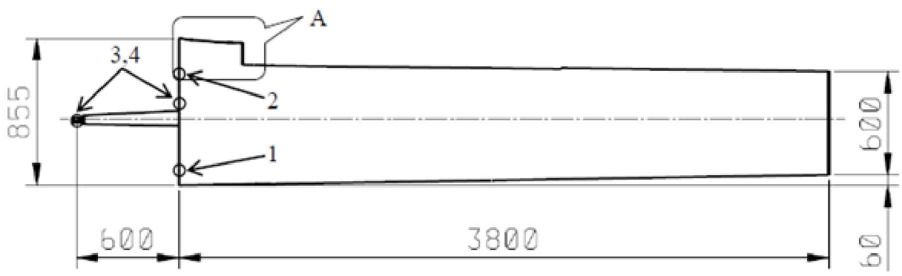

Figure 2: HpH wing top view.

To simplify the FE model, the area 'A' from Fig. 2 is excluded. Since the transition between flaperon and main part of the wing does not belong to the supporting structure, it has been also excluded. Another reason to leave out this area is due to the manufacturing process of winding. This way a new cross section of the wing has been created (Fig. 3).

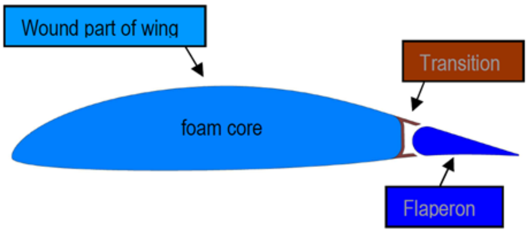

Figure 3: Simplified cross section.

The model consists of composite wound skin, foam core and wooden ribs. The schematic drawing of the model is shown on Fig. 3 and 4.

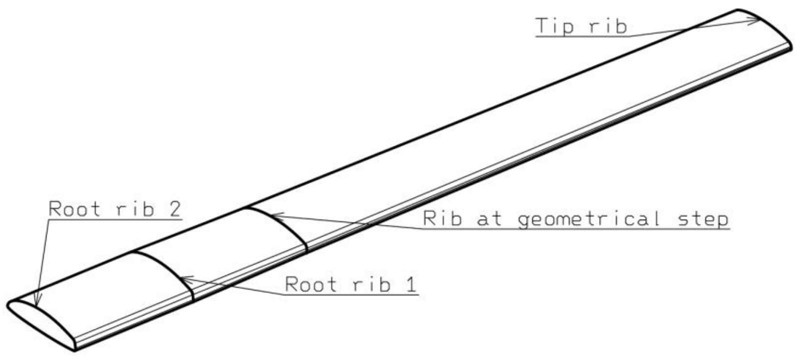

Figure 3: Schematic drawing of the segment, isometric view.

1.3 Material data

Composite materials used for finite element analysis were tested at IAE according to ASTM standards[3]. The carbon fibre properties have been measured by 4-point bend test, while the foam was tested under pressure (Fig. 5) and shear.
There were three foams (Tab. 1) selected for analysis. The foams differ in density, mechanical characteristics and price.

Property	**Foam 1**	**Foam 2**	**Foam 3**
E [MPa]	24	48	63
G [MPa]	9,8	19,6	25
σ_{Yield}[MPa]	0,85	1,6	2
P[kg*m^{-3}]	50	100	160

Table 1: Properties of foams. [IAE internal measurement].

Property	**Plywood**
E[MPa]	10000
μ[-]	0,3
t[mm]	18

Table 2: Properties of wood. [10].

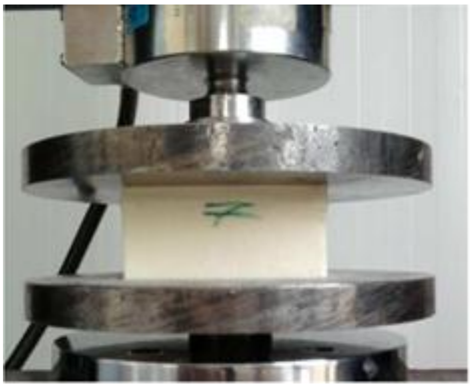

Figure 5: Foam tests: pressure.

2 Design and FE analysis

The outer shape of the wound segment is based on the real wing as described above. However the inner structure has yet to be determined. The absence of the spars is compensated by the skin itself. Since the load on the segment is mostly bend momentum and translational shear force, the main characteristic is the bend stiffness (BS) of the segment.
Finite element analysis aims to suggest how should the inner structure look like to meet the requirements (to withstand the ultimate loading taken from the real HpH wing segment.).

2.1 Analytical stiffness estimation

The bend stiffness BS [N*mm^2] is determined from geometry and material of the wing:

$$BS=EJ \qquad (1)$$

where E [MPa] is elastic modulus of the carbon fibres and J [mm^4] is cross section quadratic momentum.
Since the winding technology is capable to create only constant thickness along the wingspan, the layup will be the same on the whole wing segment, thus the E is constant as well. The BS parameter will depend on geometry (J parameter) only.

2.2 Finite element analysis

For FE analysis is used MSC.Patran/Nastran software package. The carbon skin and wooden ribs are represented by linear shell elements TRIA3 and 2D orthotropic material or isotropic respectively, whereas foam is represented by linear 3D elements CTETRA and isotropic material. Moreover the foam is defined as perfectly plastic material.
Used boundary conditions (Fig. 6 and 7) are two displacement constrains and one force load:

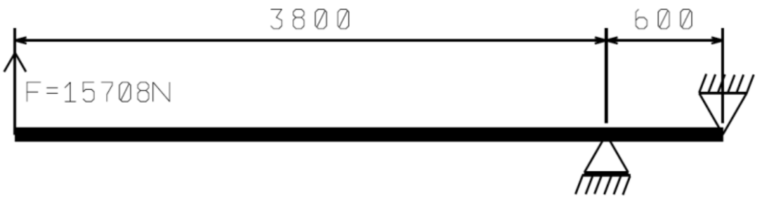

Figure 6: Boundary conditions of wing segment.

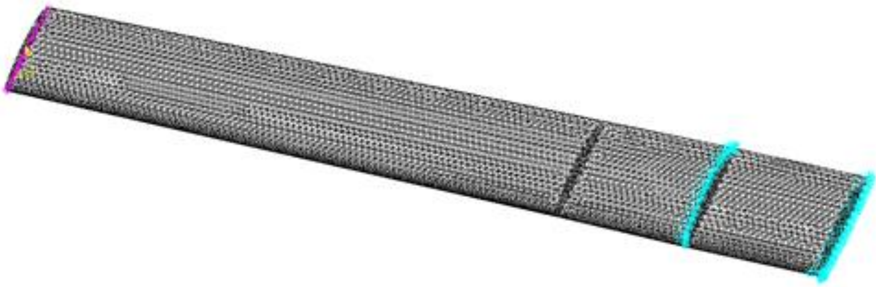

Figure 7: Finite element model of wing segment.

Non-linear solver SOL106 and OP2 output file has been chosen. It will allow to find out more details about the displacement, stresses and failure indexes.

2.3 Failure criteria

During post-processing were used the following sandwich (Fig. 8) and skin failure criteria:

- Wrinkling
- Crimping
- Shear stress
- Skin local buckling (de formation)
- Skin ply failure (max stress)

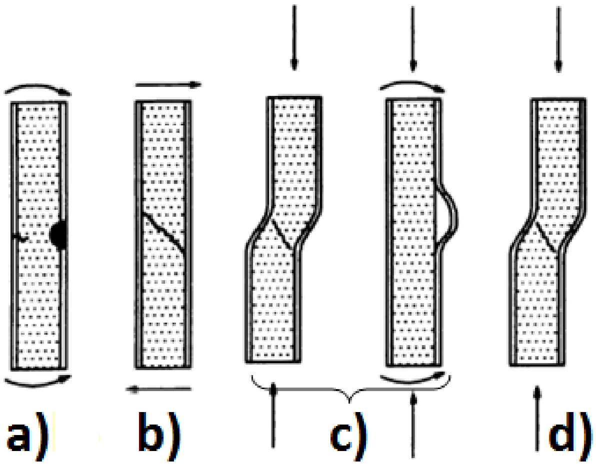

Figure 8: Sandwich failure modes: a) Outer skin failure; b) Core crack; c) Face wrinkling; d) Crimping.

Face sheet wrinkling is short local wave buckling pattern of the sandwich skin. It can buckle inwards or outwards, depending on the relative strengths of the core in compression and the adhesive in flat wise tension. The wrinkling stress is calculated according to the following equation:

$$\sigma_{wr}=k(E_f G_c E_c)^{1/3} \qquad (2)$$

where E_C [MPa] exhibits core compressive Young modulus in direction of sandwich thickness, G_C [MPa] shear core modulus, and E_F [MPa] face Young modulus in principal compressive stress direction. Wrinkling factor k [-] depends on core thickness (foam core k = 0.76, multi-web k = 0.63)[2].

The shear crimping is caused by low core shear modulus, or low adhesive shear strength. The generic relation

$$N_{cr}=G_c\,t \qquad (3)$$

was adopted from literature [3]. The value NCR [N/m] represents force per length unit and t [mm] is core thickness.

Shear core strength was evaluated directly from von Misess stress result on volume elements. For further comparison a global stiffness GS [N*mm] has been introduced:

$$GS=F/D \qquad (4)$$

where F [N] is the force applied and D [mm] is segment's tip displacement.

2.4 Results of FE analysis

The problematic part is upper surface (compression loading), where the foam is crashed by the skin wrinkles. Once the foam is crashed, the complete destruction occurs. Analysis showed large dependence of failure point on the foam stiffness (Fig. 9, Tab. 3).

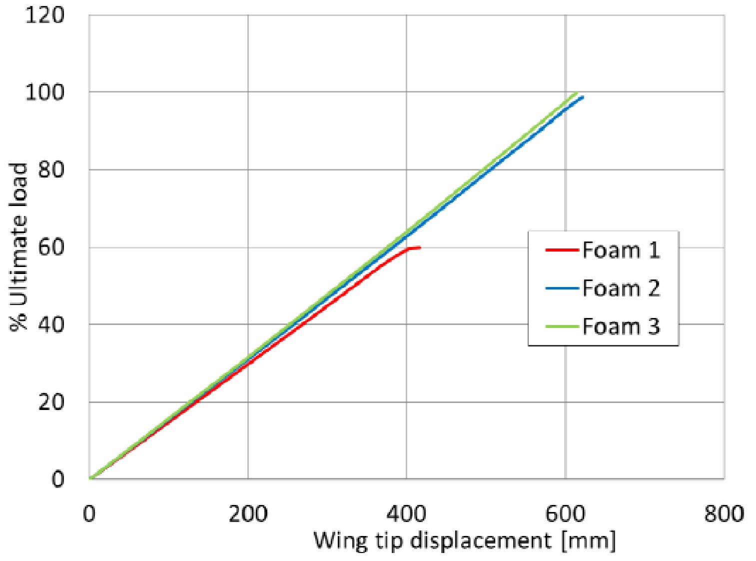

Figure 9: Dependence of ultimate load on the segment's tip displacement.

	Foam 1	Foam 2	Foam 3
Failure	**Ultimate load** [%]		
Wrinkling	50	76	91
Crimping	X	X	X
Core shear	60	98	X
Local skin buckling	57	97	X
Composite skin failure	58	98	X

Table 3: Percent of the ultimate load when given failure occurred.

	Foam 1	Foam 2	Foam 3
Global stiffness GS [N/mm]	23,5	25,0	25,6
Weight [kg]	25,5	35,3	47,1

Table 4: Comparison parameters: Global stiffness and weight of the segment.

2.5 Multi-web structure

To reduce the weight and to redistribute translational shear force a multi-web structure has been proposed. This design uses milling on larger scale then the foam core design.
Multi-web structure (Fig. 10) consists of several handmade spars. These spars are supposed to be loaded by translational shear force and ease up the skin and core load. Such construction is bend-stiffer (the ratio displacement vs. load) then previous foam-core design.
The boundary condition, material characteristics and the layers are the same.

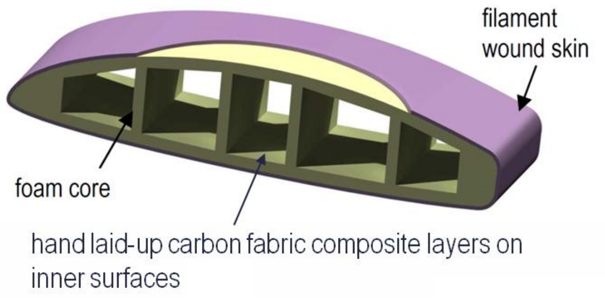

Figure 10: Proposed multi-web inner design.

The Fig. 11 shows some non-linear behavior of the model. This is caused by foam creeping. In previous model, foam core structure, the point of failure occurred simultaneously with the foam creep.

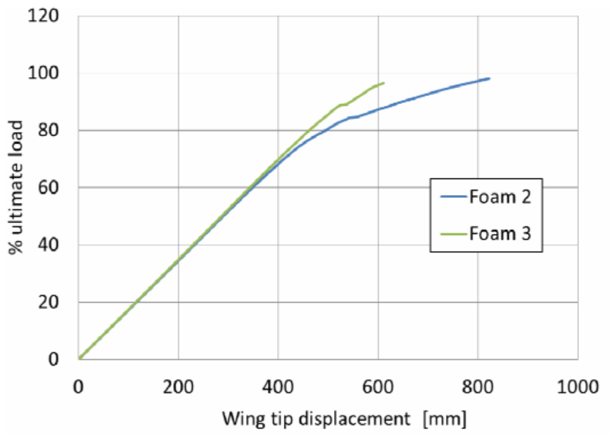

Figure 11: Dependence of ultimate load on the segment's tip displacement.

	Foam 2	Foam 3
Failure	**Ultimate load** [%]	
Wrinkling	49	58
Crimping	25	32
Core shear	63	75
Local skin buckling	55	65
Composite skin failure	72	80

Table 5: Percent of the ultimate load when given failure occurred.

	Foam 2	Foam 3
Global stiffness GS [N/mm]	27,1	27,4
Weight [kg]	28,7	33,4

Table 6: Comparison parameters: Global stiffness and weight of the segment.

The multi-web structure seems to be promising because of the light weight; however low-cost polyurethane foams used are not stiff enough. There is high sensitivity for sandwich crimping failure. Better results may be achieved through other, more expensive and heavier foams.

3 Manufacturing and testing of wound wing segment

3.1 Manufacturing

The wing segment is made of carbon fibres, wound by machine around milled foam core. The ratio between STS fibre and LG120 resin is 50%.
In the design stage, the layup consisted of 10 layers with stuck-up angle of ±14°. However the manufacturing process changed this stack-up to sequence of 2 layers with angle of ±65° and 8 layers of 0°.
The first layer was wound onto the foam core surface, spread by the adhesive to firmly interconnect the foam core and fibres.
The winding process progressed slower than expected, resulting in premature curing. Therefore the resulting surface became rougher and had to be repaired by spreading the resin over the surface. Finally, the segment was cured at temperature of 100°C.

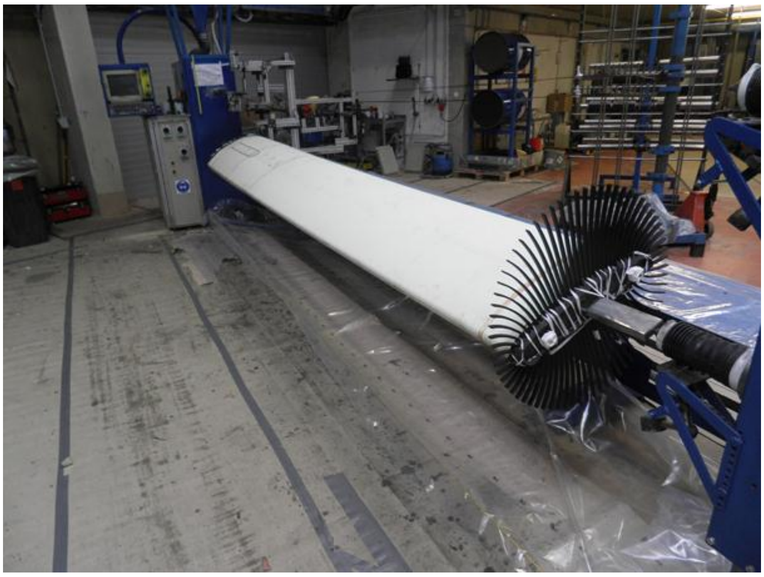

Figure 12: Winding machine and wing segment.

3.2 Testing

The segment was fixed (Fig. 13) in the area of root rib and the rib extension. Loading force was applied at the tip of the segment. During the test were measured parameters of displacement and strains at pre-defined locations. The segment has not been tested up to ultimate load in order to prevent any damage to the specimen.

Figure 13: Testing of the segment.

The result of the test has been compared (Fig. 13) to the revised (thickness and stuck-up angles) simulation in order to prove the quality of wound skin and the design itself.

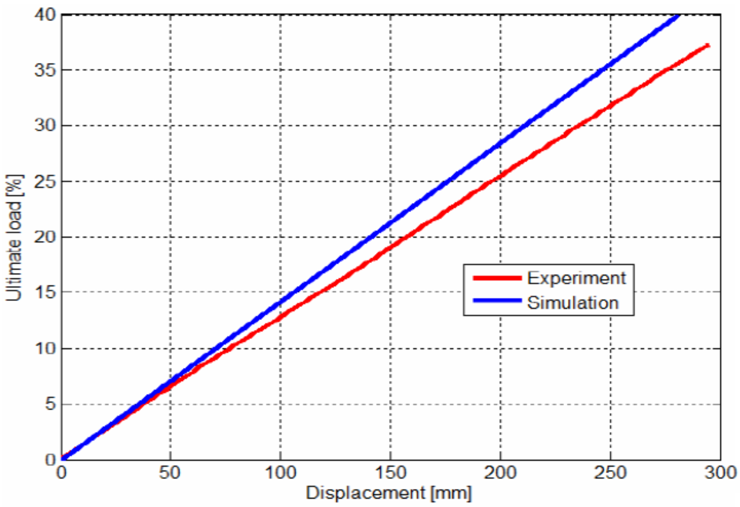

Figure 14: Comparison of test and FE analysis. Dependence of ultimate load on the segment's tip displacement.

Force and displacement dependencies measured during experiment and from FE simulation on wing tip are compared (Fig. 14). The difference in global stiffness characteristic (ratio between force and displacement) is 14.5%.

4 Future development

On previous pages were investigated options of foam-based core and filament skin wing design. No design proposed is satisfactory enough to be used in real airplane construction. However the filament placement is promising technology and new proposals arose and are investigated.
During previous foam-based designs has been expected extended usage of milling for its availability. In honeycomb-based structure is the position of milling diminished. It is worth mentioning that the price of honeycomb is at the same level like in the case of hi-quality foams. Honeycomb skin consists of 10 carbon layers ±14° one honeycomb layer and 2 closing ±45° layers.
The single spar is one honeycomb layer 15mm thick with symmetrical stuck-up of 3 carbon ±45° layers on each side.

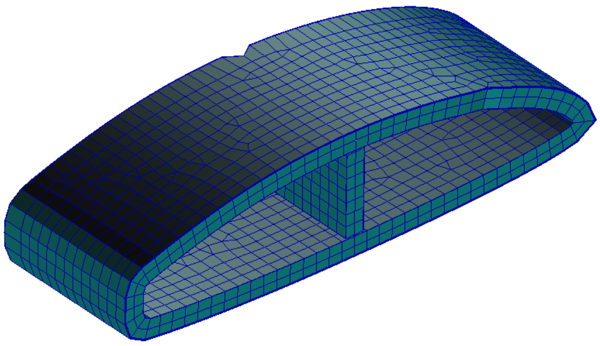

Figure 15: FE model of honeycomb segment.

Hexagonal aramid honeycomb HRH-10-3/16-6.0 from HEXCEL has been chosen.

Propety	**Honeycomb**
Cell size [mm]	4,76
E_{11} [MPa]	0,1
E_{22} [MPa]	0,1
μ [-]	0,3
G_{12} [MPa]	0,1
G_{13} [MPa]	89
G_{23} [MPa]	45
XT [MPa]	1
XC [MPa]	1
YT [MPa]	1
YC [MPa]	1
ILSS [MPa]	58
t [mm]	25

Table 6: Properties[6] of honeycomb HRH-10-3/16-6.0.

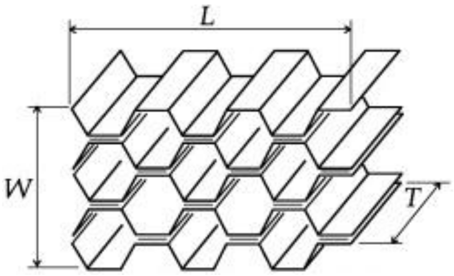

Figure 16: Honeycomb directions. LT plane corresponds to 13 plane. WT plane corresponds to plane 23.

As the simulation showed, the orientation of the honeycomb (W and L directions, Fig. 16) plays its part. There are no significant skin wrinkles, the honeycomb core is undamaged. Maximum pressure (Fig. 17) in fibres does not cause any failure.

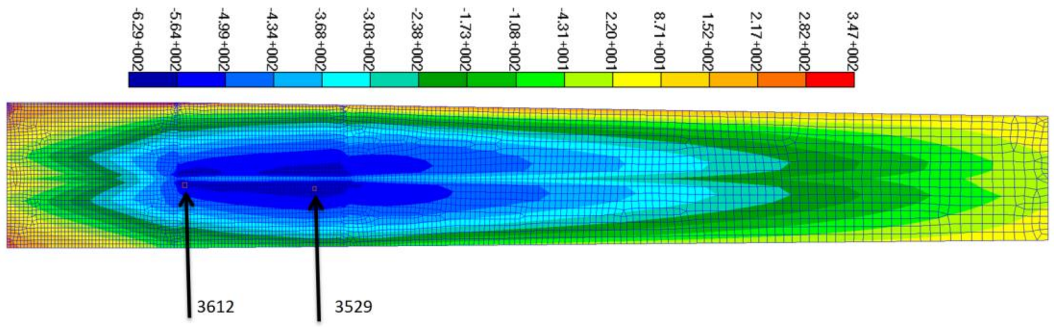

Figure 17: Normal stress σ_{11} [MPa] in fibre direction at ultimate load. Top (pressure) side of the segment. Two elements for further analysis (3612 on the left, 3529 on the right) were selected.

Two finite elements were analysed further in COMPOST[1]. Results are shown in Tab. 8.

Element	3612	3529
Core Crushing	0,76	0,76
Core Crimping	0,52	0,52
Core Shear Strength	0,12	0,05
Wrinkling Top side	0,06	0,06
Wrinkling Bottom side	0,70	0,70
Dimpling Top side	0,02	0,02
Dimpling Bottom side	0,02	0,02
TsaiHill	0,64	0,42

Table 8: Failure index for selected elements and failure criteria.

Global stiffness GS [N/mm]	26,2
Weight [kg]	28,8

Table 9: Comparison parameters: Global stiffness and weight of the segment.

[1] COMPOST is an open-source software under development at IAE. It serves for rapid post-processing of the FEM results of composite structures. The program is designed to show all important 2D elements results from MSC.Nastran.

The design described above seems to be promising as a good start for weight/strength optimization and further investigation. The first optimization might be step-thinning of the honeycomb core along the wingspan. Another optimization parameter might be the carbon stuck-up (number and span of the layers).

5 Conclusion

Parametric study of mandrel design has shown that low cost polyurethane foams are not stiff enough for applications in combination with high stiffness and strength carbon fibre laminates. When new manufacturing technology of non-constant thickness has been proposed, new analysis has been done. It did not prove any significant improvement in failure characteristics of the segment.

The compact sandwich structure using lightweight foam is prone to sandwich short wave buckling failure and shear core failure. The core in compact sandwich with desired mechanical properties is not applicable for weight reasons.

Proposed foam core segment has been manufactured. Several problems occurred during segment winding. Most of them were caused by the novelty of filament winding process in wing production. Technological problems like premature curing can be solved. Precision of filament placement and automation of wing manufacturing are very promising for future applications.

From the foam core design has been derived multi-web and honeycomb core design. The most promising variants is the honeycomb core

At the end of this paper is suggested basic idea of wound wing segment based on honeycomb core. Two optimization parameters (honeycomb thickness and carbon layers' size) are pointed out for further analysis.

The final conclusions of this paper are:

1. Analysis of wound wing segment showed that low cost polyurethane foams are not stiff enough for applications in combination with high stiffness and strength carbon fibre laminate.
2. The compact sandwich structure using lightweight foam is prone to sandwich short wave buckling failure and shear core failure.
3. Core of compact sandwich configuration which would be stiff enough for carrying desired loading is not applicable because of increased weight and cost.
4. Filament placement and automation of wing manufacturing are very promising for future applications. Technological problems will be solved.
5. From the three concepts of wound wing inner structure is the honeycomb core the most promising and will be investigated further.

Acknowledgment

Firstly our acknowledgement belongs to Compotech Plus s.r.o. and HpH Ltd. because this research could not be possible without their support during development and manufacturing of innovative sailplane wing concepts.

Also the authors would like to thank Brno University of Technology for funding of this project.

References

[1] Dimensionierungsrichwerte fur den Segel und Motorsegelflugzeugbau. Interessengemeinschaft Deutscher Akademischer Fliegergrupen, 3. 1988.

[2] Ley R.P., Lin W. Mbanefo U. Facesheet Wrinkling in Sandwich Structure. NASA/CR-1999-208994, 1999.

[3] ASM Handbook volume 21 - Composites. ISBN 0-87170-703-9, 2001.

[4] DoD Handbook Composite Materials Handbook. MIL-HDBK-17. Volume 1-3, 2002.

[5] Lopes C. S. Progressive failure analysis of towplaced, variable-stiffness composite panels. International Journal of Solids and Structures 44, 8493-8516, 2007.

[6] Hexcel.com HexWeb HRH-10 Aramid Fibre/Phenolic Honeycomb. Product data. 2012.

[7] Malis, Urik, Uher. The CFRP sailplane wing segment manufacturing by filament placement. ICAS 2012, 2012.

[8] Chvojka. HPH experimental Wing Report. Compotech, Internal Ref. No. 1434, 2012.

[9] Malis. Navrh konstrukce protoypu navijeneho kridla. BUT-FME-IAE, LU44-2012-OST.ST, 2012.

[10] Kretschmann. Wood handbook FPLâ˘A ¸SGTRâ˘A ¸S190, Wood as an Engineering Material. U.S. Department of Agriculture, Forest Service, Forest Products Laboratory: 508 p. 2010